Semina Ciências Exatas e Tecnológicas

e-ISSN 1679-0375
ENGINEERING

ORIGINAL ARTICLE DOI 10.5433/1679-0375.2026.v47.52516

iThenticate

Wear on Common Brass and Aluminum by Cavitation

Desgaste no Latão Comum e no Alumínio Devido à Cavitação

Gil Bazanini[1], Ricardo Kirchhof Unfer[2]

Received: March 17, 2025 *Received in revised form: February 23, 2026* *Accepted: March 5, 2026* *Available online: April 24, 2026*

ABSTRACT

Damages by cavitation are responsible for greater costs to the machine hydraulics industry. To study the effects of the collapse on a solid surface, a rotating disk test rig was used here to create cavities (or bubbles) in water. In the apparatus, these cavities are led to collapse on the surface of common brass and aluminum specimens. After that, the specimens are observed with the aid of a scanning electron microscope (SEM), where the damages on the specimens are analyzed, showing pits and approximate circular areas on their surfaces. An explanation is presented here for the pits, as well as images of the specimens before and after the collapses. The pits are certainly made by liquid hot micro-jet impingement resulting from the cavity in the final stages of its collapse, on the specimen surface, associated with pressure waves resulting from bubble oscillations. Damages on brass were evaluated by mean depth penetration, volume loss, volume loss rate and mass loss rate. The results are compared with the results of the available bibliography, from the 1980s until today. All specimens tested showed some kind of surface damage, such as pits and small craters resulting from cavitation. The results obtained here are very close to the ones obtained by other researchers for the brass and the aluminum specimens, respectively, despite the test rig used. Some new calculations were performed here to better justify the experimental results.

keywords wear, plastic deformation, cavities, erosion

RESUMO

Latão comum e alumínio comercial foram ensaiados utilizando o dispositivo a disco rotativo com o objetivo de se observar os efeitos da cavitação. O estudo justifica-se devido aos prejuízos causados pelos efeitos da cavitação na indústria de equipamentos e instalações hidráulicas. Foram obtidos erosão e *pits* de cavitação. Estes *pits* puderam ser observados com auxílio de um microscópio eletrônico de varredura. Pelo fato de serem causados por micro-jatos, que são conduzidos através das cavidades, ou bolhas em formato toroidal em colapso, os *pits* e demais danos apresentam formato aproximadamente circular. Uma explicação é apresentada para os *pits* bem como para as crateras resultantes do fenômeno da cavitação. O desgaste é avaliado através da penetração média nos corpos de prova, e perdas de volume e massa de material. Os resultados são comparados com resultados disponíveis na literatura desde os anos 1980 até trabalhos mais recentes. Todos os corpos de prova ensaiados apresentaram algum tipo de desgaste superficial, tais como *pits* e pequenas crateras resultantes da cavitação, compatíveis com os resultados de outros pesquisadores. Alguns resultados teóricos foram obtidos e incluídos para melhor embasar os resultados experimentais.

palavras-chave desgaste, deformação plástica, cavidades, erosão

[1]Prof. Dr., Department of Mechanical Engineering, UDESC, Joinville, SC, Brazil. gil.bazanini@udesc.br
[2]Prof. Dr., Department of Industrial Technology, UDESC, São Bento do Sul, SC, Brazil. runferengenharia@gmail.com

Introduction

Cavitation has been studied from the years of World War II with underwater explosions (Herring, 1941) until today, without complete elucidation of the phenomenon.

Damages by cavitation are responsible for greater costs to the machine hydraulics industry. Although the use of more resistant materials, such as stainless steel, may reduce the erosion progress in rotors of pumps and turbines (Moreira et al., 2023), a better understanding of the phenomenon and its damage mechanisms might reduce such costs, either for the manufacturers, or for the customers. The most usual example is the cavitation erosion in centrifugal pumps (Hattori & Kishimoto, 2008). An already known damage mechanism is mostly by liquid micro-jets impingement (Bazanini et al., 2018) and pressure waves on a solid surface. The pressure waves are caused by bubble collapse and rebound relatively far from the solid surface.

In the final stages of the collapse, as the cavity starts to deform its original shape, a water micro-jet is formed through the cavity and hits the solid surface, sometimes even removing material from the surface. The micro-jet with a velocity of approximately 100 m/s is responsible for the pit formation at the center of the cavity. After that, the cavities usually move toward the solid surface and impact it before disappearing (Brennen, 1995). Then, occurs the cavity implosion, or oscillation, causing shock and pressure waves. The bubble also releases its contents in the form of hot micro-jets on the solid surface of the specimen, creating residual stresses which are opposite to the working stresses, resulting in plastic strengthening.

To study the cavitation process and related effects, some test rigs have been developed recently, such as the impinging jet test case (Schreiner et al., 2023) and the spray jet erosion test facility (Fujisawa & Aihara, 2023). These devices consist of water liquid jets impinging on fixed test specimens. To reduce the time of the experiments, it was designed an ultrasonic test rig (Hegde et al., 2023).

There is the vertical rotating disk, see Cheng et al. (2013), for an example, where a disk with the specimens fixed on it is rotating in water to provide the cavitating flow. It should reproduce well the phenomenon of the flow through a pump, since the chamber is assembled in the place of the centrifugal pump. There is also the horizontal rotating disk test rig, Figure 1.

Figure 1 - The rotating disk test rig.

Although water tunnels (Krella et al., 2023) and vibratory devices (Dular et al., 2006), have been used for cavitation studies, the rotating disk test rig reproduces remarkably well the phenomenon. The present test rig leads the cavities to collapse over the specimens due to a system of eight baffles. The baffles are kept at a distance of 18 millimeters (mm) from the rotating disk surface containing the specimens.

The phenomenon has also been studied with the aid of high speed cameras by Dular et al. (2018), studying the collapse of a single bubble with a diameter of 5 mm. It was observed the deformation without mass loss of a thin aluminum foil for various distances of the bubble from the specimen. Using commercial software and experiments in a test pump with impeller made of aluminum, Nohmi et al. (2021) showed good agreement with the area of cavitation aggressiveness. Paquette et al. (2018) performed numerical simulations of a single air bubble collapse close to an aluminum specimen with a CFD code. It was obtained a plastic deformation of 112.2 nm.

Materials and methods

The test rig in Figure 1 shows the chamber. On the disk surface the specimens are assembled close to the cavity inducers.

The peripheral velocity is a function of the specimen position on the disk, since the rotation was kept constant at 4400 rpm, resulting in a peripheral velocity of 37 meters per second at a distance of 80 mm from the center. The disk was designed with many possibilities of distance to the center and specimen diameters for the tests, as can be seen in the schematic drawing in Figure 2.

Figure 2 - Schematic drawing of the rotating disk. Dimensions in mm.

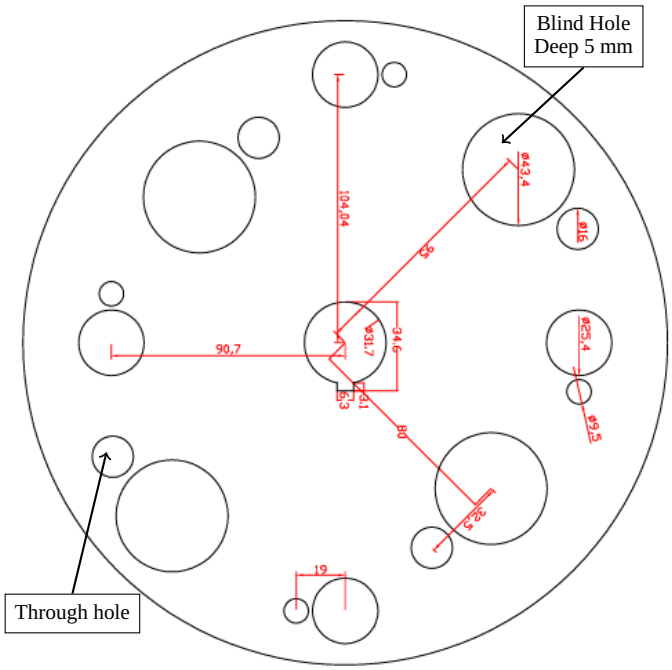

Here, we worked with the option of the distance of 80 mm from the specimens to the center of the disk to obtain the desired velocity. In the present work, brass and aluminum were used as test specimens, tested for 5, 10, 15 and 25 hours. Their chemical composition is listed in Table 1.

Table 1 - Chemical composition of test specimens (mass %).

Element (%)	Al	Brass
C	–	–
Si	0.451	0.030
Mn	0.216	0.0085
Cu	0.160	71.278
Sn	0.0010	0.2361
Al	98.200	0.0160
Pb	0.0072	1.6012
Fe	0.224	0.3165
Mg	0.683	–
Zn	0.0165	23.338

The specimens can also be seen in Figure 3. They were weighed in a digital balance accurate to 0.1 mg to obtain the mass loss in the process. Lastly, the results obtained here are compared with the ones available in the references, from the 1980s until today.

Figure 3 - Test specimens.

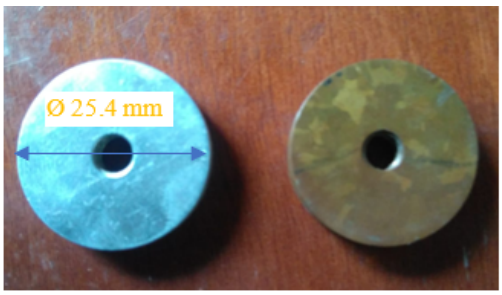

Images of the specimens were observed by the scanning electron microscope (SEM) after the tests to visualize the damages, either plastic deformation (on aluminum), or craters (on brass).

Damages on brass specimens were evaluated based on the cumulative volume loss (CVL) of material, the volume loss rate (VLR), the mean depth penetration (MDP), the mass loss rate (MLR) and the mean depth penetration rate (MDPR), in comparison with other researchers' results. Calculations of the micro jet energy were performed at the end of the next section for comparison purposes with the experimental results.

Results and discussion

After the tests under cavitating conditions using the rotating disk test rig, the pits resulting from associated phenomena such as micro-jets, high temperature and pressure waves (not directly detected) could be observed on the test specimen.

In Figure 4 it is possible to see the respective almost circular pits on the aluminum, very similar to those recently obtained by Kulmann et al. (2023), who worked with cylindrical specimens of a diameter of 12 mm and a thickness of 7 mm.

Figure 4 - Aluminum test specimen showing plastic deformations: (a) after 5 hours of tests; (b) after 10 hours of tests.

(a) (b)

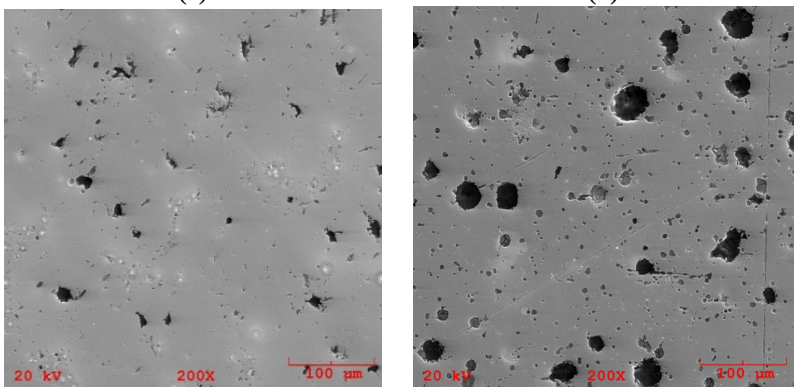

These approximate circular areas due to cavity impaction could be seen in the images after 5 hours of operation of the test rig for aluminum specimens.

For a better view, the "pits" and rings were observed by scanning electron microscope, for the tested aluminum specimen. Carbon steel was also tested by Bazanini and Bressan (2017). No significant mass loss was observed for the aluminum specimen. However, plastic strengthening was probably due to plastic deformation.

Those cavities collapsing near specimen surfaces, led to cavitation damage, not necessarily with mass loss (Chen et al., 2009). After 10 hours it was possible to see the damages caused by cavitation on the specimens. In the aluminum specimen, the pits due to liquid micro-jet impingement occur due to plastic deformation.

For the brass specimens, on the other hand, it was observed crater formation associated with mass loss. To measure the damages, it was used here the concepts of cumulative volume loss, volume loss, the mean depth penetration and the mean depth penetration rate. The variables were determined from Figure 5 and also obtained with scanning electron microscope images.

Figure 5 - Brass test specimens: (a) after 5 hours of tests; (b) after 10 hours of tests; (c) and (d) after 15 hours of tests.

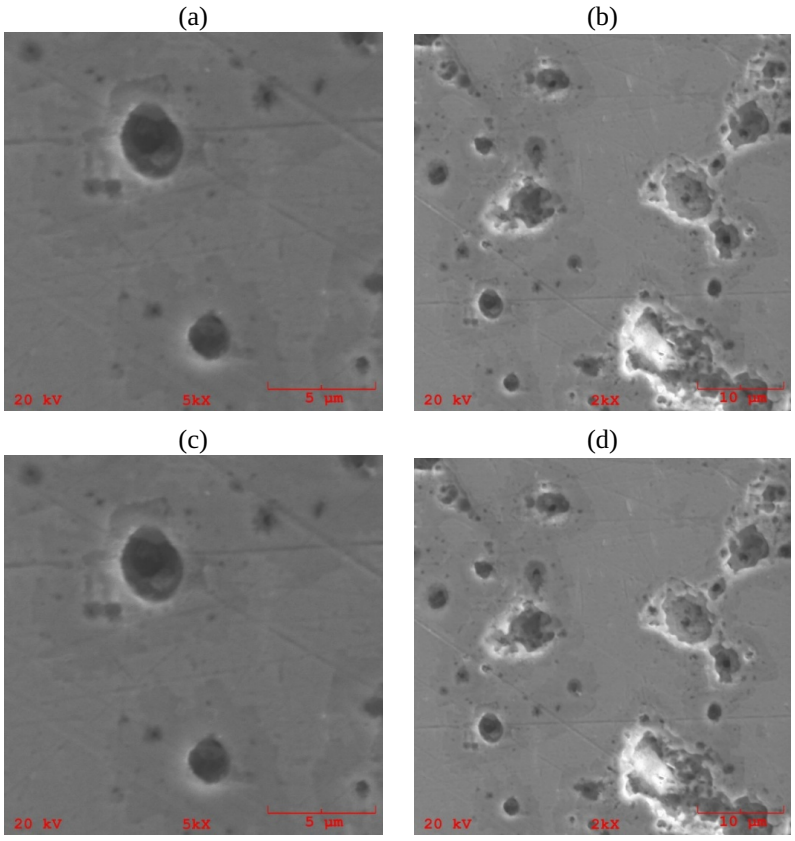

So, the damages were formed as cavitation pits in the aluminum specimens. They are created by several mechanisms, such as micro-jets and pressure waves, which have resulted from the cavity collapse process and from plastic surface deformation, resulting in damaged areas. A theoretical description of the cavity collapse can be seen in Bazanini and Bressan (2017).

In their most recent work, Kulmann et al. (2023), making experiments with laser-induced single cavitation bubble radius of 1.2 mm recorded by two high speed cameras also did not observe significant mass loss in their pure aluminum specimen tested. Instead, they obtained protruding pits very similar to the ones obtained by Bazanini et al. (2018).

In fact, aluminum was already tested for a period of just 5 hours with the rotating disk rig without significant mass loss by Bazanini et al. (2020), but damages such as ellipsoidal pits.

Data of mass loss for the specimens are shown in Table 2 for the aluminum and in Table 3 for the brass.

Table 2 - Mass loss for the aluminum (2 specimens).

Time of tests (hours)	Mass (g) (Specimen 1/2)	Cumulative mass loss (g)
0	6.3304 / 6.2160	-
5	6.3288 / 6.2160	1.6E-3 / 0.0000
10	6.3288 / 6.2157	1.6E-3 / 3E-4
Average mass loss (g)		9.5E-4

With these samples it was possible to evaluate the mass loss rate, the cumulative volume loss, the volume loss rate and the mean depth penetration as follows, in comparison to other researchers' results.

Table 3 - Mass loss for the brass (1 specimen).

Time of tests (hours)	Mass (g)	Cumulative mass loss (g)
0	19.9629	-
5	19.9567	6.2E-3
10	19.9514	0.0117
15	19.9441	0.0188
25	19.9267	0.0362

For the brass, the mass loss rate is shown in Table 4 with the water velocity of the tests, and the other parameters (cumulative volume loss, volume loss rate and mean depth penetration along with the water velocity) are shown in Table 5. For the aluminum, the results appear in Table 6.

Table 4 - Mass loss rate (MLR) and water velocity (V) after 5 hours of tests for brass specimens

Author	MLR (mg/min)	Time of tests (hours)	V (m/s)
Present work	0.021	5	37
Zhiye (1983)	0.025	3.3	43.2

Table 5 - Cumulative volume loss (CVL), volume loss rate (VLR), mean depth penetration (MDP) and water test velocity (V) for the brass, present work/Rao et al. (1980), except*

Time (hours)	CVL (mm^3)	VLR (mm^3/h)	MDP (mm)
10	1.35 / 1.67	0.135 / 0.167	-
15	2.2 / 1.5	0.145 / 0.10	-
25	4.26 / 5.0	0.17 / 0.20	-
25	-	-	0.03 / 0.032
*104; Schreiner et al. (2023)	-	-	0.07
Time (hours)	**V (m/s)**	**Test rig**	**Material**
10	37 / 36.6	Rotating disk	Brass
15	37 / 53.8	Rotating disk	Brass
25	37 / 53.8	Rotating disk	Brass
25	37 / 37.3	Rotating disk	Brass
*104; Schreiner et al. (2023)	-	Jet test case	Ductile steel

Table 6 - Cumulative mass loss (CML) and cumulative volume loss (CVL) for the aluminum.

Author	CML (mg)	Time of tests	Test rig	CVL (mm^3)
Present work	0.95	10 hours	Rotating disk	-
Hegde et al. (2023)	1	42 min	Ultrasonic test rig ASTM G32-16	-
Fujisawa and Aihara (2023)	-	Flow volume: 0.6×10^5 mm^3	Droplets impacts	1

An interesting parameter of analysis is the mean depth penetration rate (MDPR) that is basically the MDP per unit time. For the experiments performed here, from Table 5, the MDPR for the brass will be $0.03/25$, that is, 1.2×10^{-3} mm/hr.

Although the test velocity of Rao et al. (1980) varied from 36.6 m/s to 53.8 m/s, see Table 6, they worked with specimens of a diameter of 63.5 mm, greater than the ones used in the present work, that is, 25.4 mm. That explains the differences in the results observed. Zhiye (1983) experiments were performed in a shorter period of time, the water velocity is greater than the one used here, which explains the slightly greater value of mass loss rate obtained.

The similarity in the results is explained by the fact that, although Hegde et al. (2023) tests were performed for a period of only 42 minutes, they used a test rig that accelerates the process, although does not reproduce quite well the flow through a pump (in the present work, the pump was replaced by the chamber with the disk with the specimens fixed on it).

Working with an impinging jet test case and using a disk of 30 mm of ductile steel, Schreiner et al. (2023) measured an erosion depth of about 0.07 mm after 104 hours of tests. Although this value is greater than those of Table 5, it is not possible to make effective comparisons due to the differences between the test rigs configurations, materials and test times, which, in that case, are much longer than in the present work, thus leading to greater values of damage.

Fujisawa and Aihara (2023) studied the pit formation from droplets impacts with a velocity of 140 m/s (greater than the velocity of the microjets which is about 100 m/s) on half cylinder targets on aluminum, obtaining final values of the order of 1 mm^3 cumulative volume loss, depending on the shape of the half cylinder. But it is not possible to make an accurate comparison with the other researchers of Table 5 and Table 6 due to the differences between the processes or materials. Besides, they set a volume flow of droplets of 0.6×10^5 mm^3.

Considering a water density ρ of 1000 kg/m^3 and a micro-jet velocity V of 100 m/s, the pressure energy of a micro-jet is:

$$E_{Pr} = \rho V^2 = 10^7 \text{ Pa} = 0.01GPa. \tag{1}$$

An equation to calculate the energy of deformation in metals is:

$$\int \sigma \, d\varepsilon \approx \frac{\sigma_y + \sigma_u}{2} \varepsilon, \tag{2}$$

where σ_u denotes the ultimate strength, equal to 90 MPa for aluminum and 350 MPa for brass; σ_y denotes the yield strength, equal to 30 MPa for aluminum and 150 MPa for brass; and ε represents the deformation.

Using a typical deformation of 0.35 for both aluminum and brass and performing the calculations with equation (2), a specific energy of deformation of 0.021 GPa for aluminum and 0.087 GPa for brass is obtained, of the same order of magnitude as the energy of a single micro-jet. However, in the cavitation cloud there are thousands of micro-jets impinging on the specimen surface during the test period, resulting in deformation of aluminum and brass in the form of pits. The excess energy is possibly required due to plastic strengthening of the metal, and part of the energy is dissipated in the form of pressure waves in the liquid, a characteristic of the cavitation phenomenon.

For the aluminum, it was calculated the pitting rate, that is, the number of pits per area per time (Bazanini et al., 2018). Based on Figure 4, a pitting rate of approximately 6.25 pits per mm^2 per hour was obtained.

It was also obtained here a depth of about 0.01 mm for the pits, greater than the results of Paquette et al. (2018). That is possible due to the fact that a vaporous bubble collapse is usually much more violent than the air bubble collapse.

Conclusions

All specimens tested showed some kind of surface damage, such as pits and small craters resulting from cavitation when observed by the SEM, and justified by theoretical calculations. These cavitation pits are approximately circular since they are caused by hot micro-jets created in the final stages of the collapse of such cavities.

For the aluminum, the “circular” areas occur by bubble impression or plastic deformation leading to plastic strengthening resisting material removal and requiring an exceeding amount of energy from the microjet, since no significant mass loss was observed in these experiments for that material. So, progressive cavity collapses and their rebounds may or may not lead to fatigue failure. That resulted in damage in the incubation period, where damage is already present without material loss.

The prints may be “individual” marks, almost like an identification of each bubble, also observed by Kulmann et al. (2023), instead of the earlier belief of complete damage by fatigue failure. The fatigue may occur just in an ultimate phase of the process, when these prints are superimposed on each other.

So, such phenomenon was characterized by water micro-jets from the final stages of the cavity collapse, impaction with plastic deformation of the test specimen, together with the resulting pressure waves generated by bubble oscillation. All these facts are combined, impacting the nearby solid surface.

For the brass it was observed mass loss resulting in the formation of pits in the shape of craters. Of course, after 25 hours of testing, these craters are no longer approximately spherical. Since the brass was tested for a longer period of time, damage resulted out of the incubation period, with material loss.

Finally, when comparing all results it was also possible to observe the effect of test time by increasing the damages on the test specimens, whatever the apparatus used.

Author Contributions

G. Bazanini participated in: conceptualization, data curation, formal analysis, investigation, methodology, writing– original draft. **R. K. Unfer** participated in: supervision, validation, visualization, writing– revision and editing.

Conflicts of Interest

No potential conflict of interest was reported by the authors.

References

Bazanini, G., & Bressan, J. D. (2017). Hot vapor bubble prints on carbon steel. *Journal of Applied Mathematics and Physics*, *5*, 439–448. https://doi.org/10.4236/jamp.2017.52038

Bazanini, G., Lima, N. N. C., & Bressan, J. D. (2018). Cavities “pit number” and micro-jets impingements. *Semina: Ciências Exatas e Tecnológicas*, *39*(2), 81–86. https://doi.org/10.5433/1679-0375.2018v39n2p81

Bazanini, G., Unfer, R. K., & Lima, N. N. C. (2020). Cavitation erosion micro-jets studies of aluminum specimens with the aid of the rotating disk device. *Engenharia Térmica*, *19*, 3–6. https://doi.org/10.5380/reterm.v19i1.76422

Brennen, C. E. (1995). *Cavitation and bubble dynamics*. Oxford University Press.

Chen, H. S., Li, J., & Liu, S. H. (2009). A ring area formed around the erosion pit on 1cr18ni9ti stainless steel surface in incipient cavitation erosion. *Wear*, *266*, 884–887. https://doi.org/10.1016/j.wear.2008.08.002

Cheng, F., Jiang, S., & Liang, J. (2013). Cavitation erosion resistance of microarc oxidation coating on aluminium alloy. *Applied Surface Science*, *280*, 287–296. https://doi.org/10.1016/j.apsusc.2013.04.151

Dular, M., Pirc, Z., Požar, T., & Petkovšek, R. (2018). High speed observation of damage created by a collapse of a single cavitation bubble. In *Proceedings* [Proceedings]. 10th International Symposium on Cavitation. Maryland, United States. https://cav2018.jhu.edu/wp-content/uploads/Dular-Matevz.pdf

Dular, M., Stoffel, B., & Sirok, B. (2006). Development of a cavitation erosion model. *Wear*, *261*, 642–655. https://doi.org/10.1016/j.wear.2006.01.020

Fujisawa, N., & Aihara, A. (2023). Rain erosion mechanism on a leading-edge half cylinder. *Wear*, *532–533*. https://doi.org/10.1016/j.wear.2023.205103

Hattori, S., & Kishimoto, M. (2008). Prediction of cavitation erosion on stainless steel in centrifugal pumps. *Wear*, *265*(11/12), 1870–1874. https://doi.org/10.1016/j.wear.2008.04.045

Hegde, M., Mohan, J., Warraich, M. Q. M., Kavanagh, Y., Duffy, B., & Tobin, E. F. (2023). Cavitation erosion and corrosion resistance of hydrophobic sol–gel coatings on aluminum alloy. *Wear*, *524–525*, 204766. https://doi.org/10.1016/j.wear.2023.204766

Herring, C. (1941). *Theory of the Pulsations of the Gas Bubble Produced by an Underwater Explosion* (Report No. 236). Office of Scientific Research and Development, Columbia University.

Krella, A. K., Grześ, J., Erbe, A., & Folstad, M. (2023). Behaviour of nickel coatings made by brush plating technology in conditions of cavitation erosion and corrosion. *Wear*, *530–531*, 204998. https://doi.org/10.1016/j.wear.2023.204998

Kulmann, J., Lozano, C. L. A., Hankes, S., & Kaiser, S. A. (2023). Correlation of laser-induced single bubbles with cavitation damage via in-situ imaging. *Wear*, *522*, 204723. https://doi.org/10.1016/j.wear.2023.204723

Moreira, C. E. S., Meinhardt, C., Caldeira, L., Oliveira, M. J. C., & Silvestre, P. (2023). Investigation of the cavitation phenomenon effect in the mechanical and metallurgical properties of the rotor of the Francis type turbine made of stainless steel ASTM A743 GR CF20. In Associação Brasileira de Engenharia e Ciências Mecânicas, *Proceedings* [Conference]. 27th International Congress of Mechanical Engineering. https://doi.org/10.26678/ABCM.COBEM2023.COB2023-2115

Nohmi, M., Tsuneda, T., Kagawa, S., & Nakamoto, H. (2021). Numerical prediction of cavitation erosion in a centrifugal pump. In *Proceedings* [Proceedings]. 11th International Symposium on Cavitation. Daejeon, South Korea.

Paquette, Y., Fivel, M., Ghigliotti, G., Johnsen, E., & Franc, J.-P. (2018). Fluid-structure interaction in cavitation erosion. In Hal Open Science, *CAV2018* [Proceedings]. 10th International Symposium on Cavitation. Maryland, United States. https://hal.science/hal-01692512v1/document

Rao, P. V., Rao, B. C. S., & Rao, N. S. L. (1980). Erosion and cavity characteristics in rotating components. *Journal of Testing and Evaluation*, *8*(3), 127–142. https://doi.org/10.1520/JTE10609J

Schreiner, F., Haese, M. G., & Skoda, R. (2023). Three-dimensional flow simulation and cavitation erosion modeling for the assessment of incubation time and erosion rate. *Wear*, *524–525*, 204747. https://doi.org/10.1016/j.wear.2023.204747

Zhiye, J. (1983). *An experimental investigation on cavitation erosion for propeller alloys*. China Ship Scientific Research Center.